

The Concept of Wheeled-Legged Robot Transformation

Nuryanto¹, Andi Widiyanto¹, Oesman Raliby¹, Rochim Widaryanto¹ and Mochammad Ariyanto²

¹Engineering Faculty, Universitas Muhammadiyah Magelang, Indonesia
email: nuryanto@ummgl.ac.id, andi.widiyanto@ummgl.ac.id, Oest72@gmail.com, rochimxwidaryanto@gmail.com

²Department of Mechanical Engineering, Diponegoro University, Semarang, Indonesia; email: mohammad_ariyanto@ft.undip.ac.id

Abstract. Some exploration processes that are not possible for humans need special tools such as mobile robots. The mobile robot uses wheeled or legged robot to drive the motion. The previous research has focused on changing the shape of leg-wheel so that it is not as good as the actual model. In this study, we propose 'Karat', a mobile robot that has legs and wheels. The robot can select the type of locomotion such as using wheel or leg. The kinematics model for transforming from wheeled mode to legged mode is modelled in this study. The legged mode is activated when the legs are below the wheels. For the wheeled mode of the Karat, the forelegs will be lifted up then folded forward, while the rear legs will bend upwards. The maximum angle for transforming from legged to wheeled mode is 40° .

1. Introduction

Commonly, a mobile robot is a robot that can move around by using wheels. The type of mobile robot based on how it moves is divided into two types, namely wheel robots and legged robots [1]. A wheeled robot is used to pass flat roads, while a legged robot is utilized for areas that are bumpy or erratic. On the flat surfaces of wheeled robots, the design is easier, cheaper and energy efficient than legged robot because it has far fewer parts. A legged robot makes it possible to pass through fields that are too soft, slippery, or even rocky that wheeled robots cannot move [2].

Based on the weaknesses and strengths of each legged and wheeled robot, various studies have emerged which combine the two locomotion. Hylos (figure 1.a) is a robot that has four wheel-legs, each of which is connected with two Degree of Freedom (DOF) suspensions to pass uneven terrain [3]. Subsequent research attempted to change the wheel that could turn into a leg like. The Quattroped had four full circle wheels that could turn into four pieces half a circle as the robot's leg (figure 1.b) [4], and transformable wheel (figure 1.c) [5]. In 2006 a model of a "Reconfigurable Articulated Leg and Wheel" robot leg-wheel change in the United States was patented by Jacobsen et al. [6].

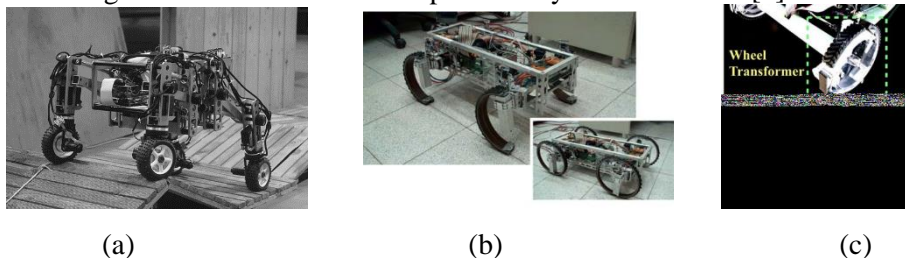


Figure 1. Wheeled-Legged Robot transformation models (a) prototype of hylos (b) The leg-wheel hybrid platform Quattroped (c) The transformable circular and legged-wheels

The proposed Karot is a mobile robot that has four legs and two wheels (2WD) in front of the body and one wheel in the rear. It works selectively based on the kind of surface. The transformation is not on the wheel-legged model, but the transformation mobile robot that can turn the model into a legged robot or wheeled robot according to the field to be passed.

2. Design of Karot

Karot uses leg and wheel locomotion that can change its locomotion according to the terrain that will be passed. Karot has two side wheels with a mad wheel on the front (2WD) and has four legs (quad pod) with the following design:

2.1. Body (Chassis)

Wheels are on the right and left sides of the robot with a rotary axis that cuts off the center of gravity as seen from the top view in Figure 2. So that the robot can rotate at the midpoint of the body without using the Omni wheel and does not change the main coordinates when changing modes. The Mad wheel is placed in the middle of the front, which later weighs the back part with other components.

The reference of the robot body is the rotating point of the servo motor whose rotary axis is perpendicular to the plane of the robot's body. Figure 2 is marked with a yellow colored circle. The four servo motors are designed to form a square with a side length a .

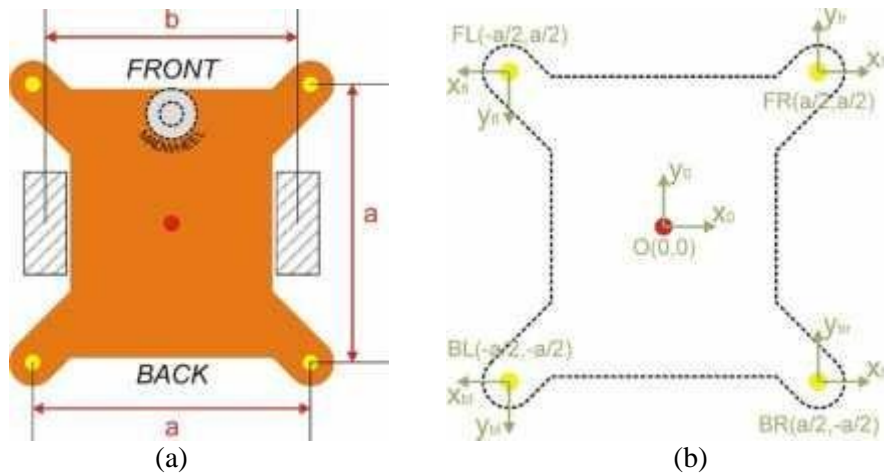


Figure 2. Design of Karot's body

The desired center of gravity for the body in Figure 2.a is marked with a red circle. The center of gravity is also at the square diagonal intersection of the four servo motors rotating points attached to the body.

The servo axis point on the body is named with the pattern to make it easier to position, F (front) or B (back) combined with L (left), and R (right). The z-axis is not included because the coordinate dimension in Figure 2.b is assumed to have the same level / Z.

The servo axis point on the body is named with a pattern to make it easier to understand the position, F (front) or B (back) combined with L (left) and R (right). The z-axis is not included because the five coordinates in Figure 4 are assumed to have the same level / Z which is the same.

Points O to each FL, BL, FR, and BR are considered passive links, so the coordinate transformations of FL, BL, FR and BR to points O (0,0,0) can be expressed as follows:

$$FL = \begin{bmatrix} x_{fl} \\ y_{fl} \\ z_{fl} \end{bmatrix}, BL = \begin{bmatrix} x_{bl} \\ y_{bl} \\ z_{bl} \end{bmatrix}, FR = \begin{bmatrix} x_{fr} \\ y_{fr} \\ z_{fr} \end{bmatrix}, BR = \begin{bmatrix} x_{br} \\ y_{br} \\ z_{br} \end{bmatrix}, \text{ and } O = \begin{bmatrix} 0 \\ 0 \\ 0 \end{bmatrix} \quad (1)$$

The mechanical manipulator consists of some body parts called links and joints. The combination is used to connect each link. Each joint represents one degree of freedom. Calculations using the Denavit and Hartenberg (DH) parameters [7] of the proposed robot's leg are shown in Table 1.

Table 1. The link-joint using DH Parameters

Link	α_{i-1}	a_{i-1}	d_i	θ_i
FL_1	0	$\frac{a\sqrt{2}}{2}$	0	135°
BL_1	0	$\frac{a\sqrt{2}}{2}$	0	-135°
FR_1	0	$\frac{a\sqrt{2}}{2}$	0	45°
BR_1	0	$\frac{a\sqrt{2}}{2}$	0	-45°

The DH parameter, a transformation matrix can be calculated as follows:

$${}^{i-1}T_i = \begin{bmatrix} \cos \theta_i & -\sin \theta_i \cos \alpha_{i-1} & \sin \theta_i \sin \alpha_{i-1} & a_{i-1} \cos \theta_i \\ \sin \theta_i & \cos \theta_i \cos \alpha_{i-1} & -\cos \theta_i \sin \alpha_{i-1} & a_{i-1} \sin \theta_i \\ 0 & \sin \alpha_{i-1} & \cos \alpha_{i-1} & d_i \\ 0 & 0 & 0 & 1 \end{bmatrix} \quad (2)$$

The transformation matrix of each servo body can be written as in (3)

$${}^0T_{FL_1} = \begin{bmatrix} -\frac{\sqrt{2}}{2} & -\frac{\sqrt{2}}{2} & 0 & -\frac{a}{2} \\ \frac{\sqrt{2}}{2} & -\frac{\sqrt{2}}{2} & 0 & \frac{a}{2} \\ 0 & 0 & 1 & 0 \\ 0 & 0 & 0 & 1 \end{bmatrix} \quad {}^0T_{BL_1} = \begin{bmatrix} -\frac{\sqrt{2}}{2} & \frac{\sqrt{2}}{2} & 0 & -\frac{a}{2} \\ \frac{\sqrt{2}}{2} & -\frac{\sqrt{2}}{2} & 0 & -\frac{a}{2} \\ 0 & 0 & 1 & 0 \\ 0 & 0 & 0 & 1 \end{bmatrix} \quad {}^0T_{FR_1} = \begin{bmatrix} \frac{\sqrt{2}}{2} & -\frac{\sqrt{2}}{2} & 0 & \frac{a}{2} \\ \frac{\sqrt{2}}{2} & \frac{\sqrt{2}}{2} & 0 & \frac{a}{2} \\ 0 & 0 & 1 & 0 \\ 0 & 0 & 0 & 1 \end{bmatrix} \quad {}^0T_{BR_1} = \begin{bmatrix} \frac{\sqrt{2}}{2} & \frac{\sqrt{2}}{2} & 0 & \frac{a}{2} \\ -\frac{\sqrt{2}}{2} & \frac{\sqrt{2}}{2} & 0 & -\frac{a}{2} \\ 0 & 0 & 1 & 0 \\ 0 & 0 & 0 & 1 \end{bmatrix} \quad (3)$$

Figure 3 is a joint angle description of the first servo angle for each leg, namely θ_{fl1} , θ_{fb1} , θ_{fr1} , and θ_{br1} . While θ_w is the angle of the first servo range in each one when walking using leg locomotion.

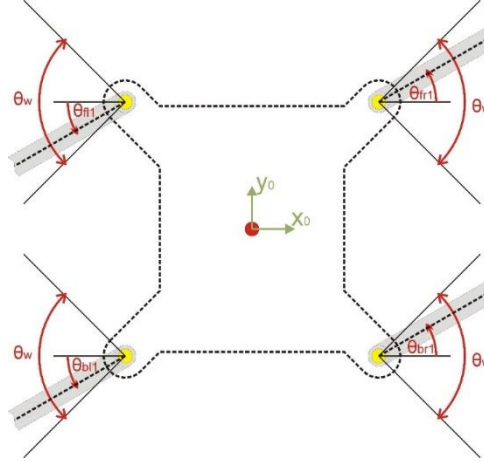


Figure 3. The formed angle by the first leg of servo motor when in the legged locomotion

2.2. Legs

Each robot's leg has the same dimensions, namely L_1 , L_2 , and L_3 . L_1 has a value of 41 mm. This value is taken because it is the smallest value so that the moment of inertia to the weight of the robot is as small as possible by looking at the dimensions of the servo motor. Assumptions of the other link dimensions are based on servo dimensions, robot dimensions and maximal torque of the servo motor. The default mode of the locomotion on the robot's leg is shown in Figure 4.a

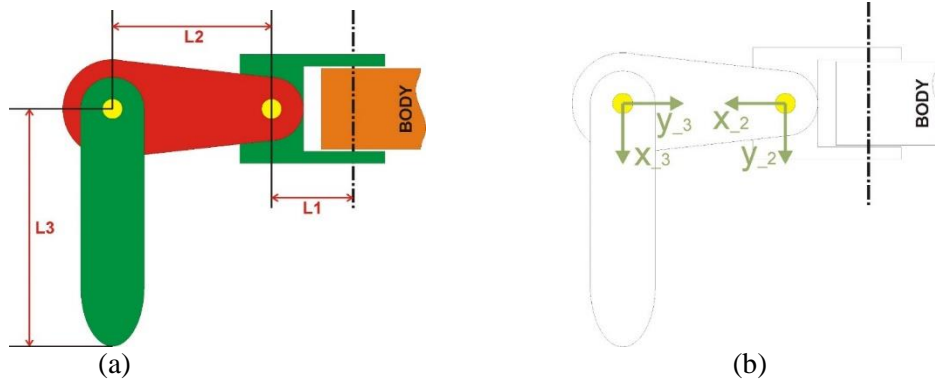


Figure 4. Leg design of Karot, (a) Dimensions of robot's leg, (b) Servo coordinate system of the robot's leg

The D-H parameter as shown in Figure 4, and the transformation matrix of each leg can be determined as shown in Table 2, Table 3, Table 4, and Table 5 respectively.

Table 2. Table link-joint of Front-Left legs

Link	α_{i-1}	a_{i-1}	d_i	θ_i
FL_1	0	$\frac{a\sqrt{2}}{2}$	0	135°
FL_2	-90	$L1$	0	45°
FL_3	0	$L2$	0	0°
FL_4	0	$L3$	0	90°

Table 3. Table link-joint of Back-Left legs

Link	α_{i-1}	a_{i-1}	d_i	θ_i
BL_1	0	$\frac{a\sqrt{2}}{2}$	0	-135°
BL_2	-90	$L1$	0	-45°
BL_3	0	$L2$	0	0°
BL_4	0	$L3$	0	90°

Table 4. Table link-joint of Front-Right legs

Link	α_{i-1}	a_{i-1}	d_i	θ_i
FR_1	0	$\frac{a\sqrt{2}}{2}$	0	45°
FR_2	-90	$L1$	0	-45°
FR_3	0	$L2$	0	0°
FR_4	0	$L3$	0	90°

Table 5. Table link-joint of Back-Right legs

Link	α_{i-1}	a_{i-1}	d_i	θ_i
BR_1	0	$\frac{a\sqrt{2}}{2}$	0	-45°
FB	-90	$L1$	0	45°
BR_3	0	$L2$	0	0°
BR_4	0	$L3$	0	90°

3. Results and Discussion

Simulation is conducted by using MATLAB/Simulink software. To speed up the modeling process, it was assembled using SolidWorks, then exported to SimMechanics toolbox under Simulink environment. The wheeled-legged robot's 3D model is shown in Figure 5, the 3D model of the robot is simplified to ease the simulation.

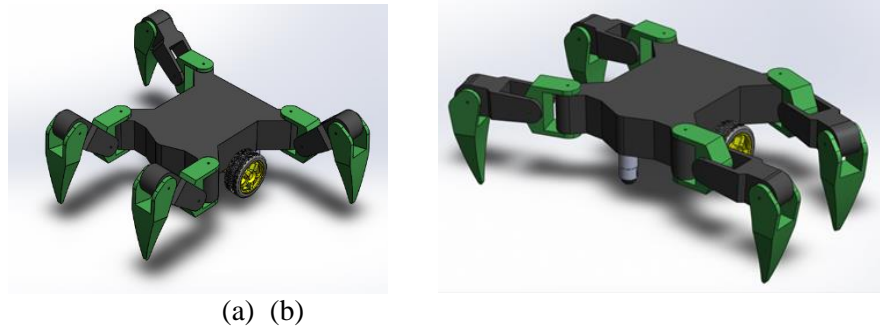


Figure 5. 3D model for simulation in CAD Software (a) wheeled mode (b) legged mode

Figure 5.a shows the default position when the robot is standing on legged mode. Whereas in Figure 5.b shows the position of the Robot's legs when the robot uses wheeled mode locomotion. The front leg protrudes forward and the back leg is in sideways. This pose aims to drag the robot's center of gravity forward so that it doesn't topple backward when driving with the wheel.

The next simulation is to determine the tip leg trajectory that is carried out by the robot's leg while walking. When pedaling to push the toe, body must be on the floor, a Cartesian motion is used to move from the starting point to the destination. While the leg movement step employs joint-space motion.

The used length of each link for simulation on the foot is as follows: $L_1 = 41$ mm, $L_2 = 80$ mm, and $L_3 = 120$ mm. Furthermore, the leg trajectory is performed using the Robotics Toolbox from Peter Corke. The setting of the foot on the robot's leg when walking is shown in Figure 6.a. In swing trajectory generation, the implemented swing angle is $\theta_w = 20^\circ$, the trajectory plot of the leg is indicated by a loosely dotted red line as shown by Figure 6.b.

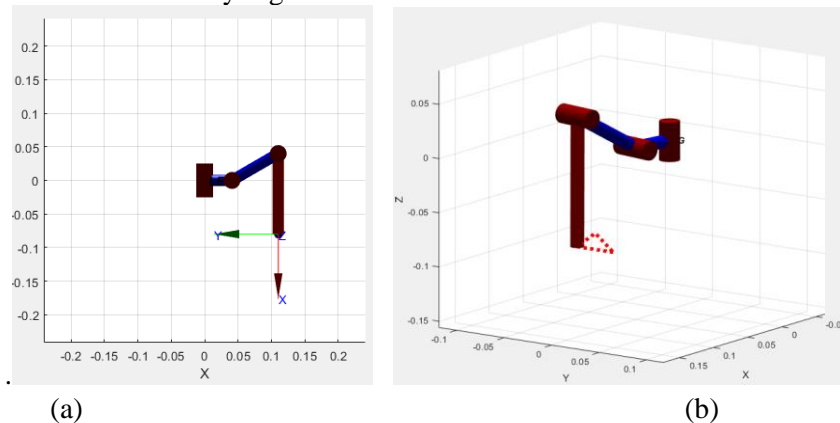


Figure 6. Peter Corke's Robotics Toolbox in MATLAB (a) Robot legs when walking (b) Trajectory plot of the leg

The dotted line that forms a triangle is the trajectory of the toe in the cycle/straight gait. The trajectory is generated by reverse kinematics using the Robotic Toolbox. The four parameter inputs are: major points are passed in the cycle of motion, time from one point to another (0.5 second interval), trajectory shape, and initial condition.

The angle of inverse kinematics result of the trajectory angle formed is then reduced to the angular angle of three servo motors. The angular angle graph of three servos is then reduced to angular angle as shown in Figure 7.

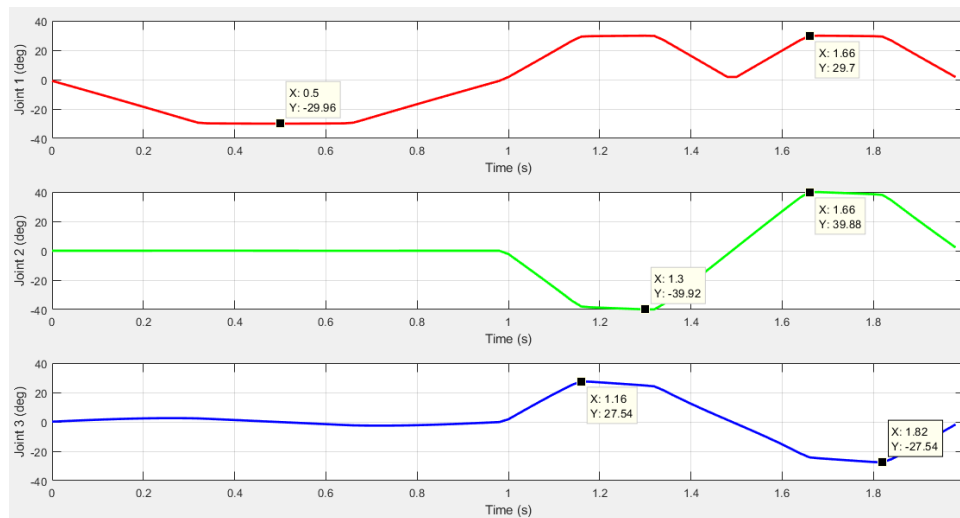


Figure 7. Angular angle graphs derived from inverse kinematics results from trajectory. Based on the figure, the values of the servo angular angle graph are presented in table 6. In order to the robot's prototype can fit with the model design, the maximum servo angular angle is 40° .

Table 6. Servo motor angular angles

Joint / Servo	Maximum of servo angular angle	Minimum servo angular angle
1	30°	-30°
2	40°	-40°
3	28°	-28°

4. Conclusion

The transformation of the wheeled-legged mode from legged to wheeled mode of the Karot, forelegs will be lifted up then folded forward, while the rear legs will bend upwards. Based on the inverse kinematics result, the needed maximum angular servo motor angle to transform from legged mode to wheeled mode is 40° .

5. References

- [1] A. Rahmawan and T. Prahasto, "Optimasi Gripper Dua Lengan dengan Menggunakan Metode Genetic Algorithm pada Simulator Arm Robot 5 DOF (Degree of Freedom)," *J. Tek. Mesin S-1*, vol. 1, no. 2, pp. 9–16, 2013.
- [2] N. B. Ignell, N. Rasmusson, and J. Matsson, "An overview of legged and wheeled robotic locomotion," 2012.
- [3] C. Grand, F. Benamar, F. Plumet, and P. Bidaud, "Stability and Traction Optimization of a Reconfigurable Wheel-Legged Robot," *Int. J. Rob. Res.*, vol. 23, no. 10–11, pp. 1041–1058, Oct. 2004.
- [4] S.-Y. Shen, Cheng-Hsin Li, C.-C. Cheng, J.-C. Lu, S.-F. Wang, and P.-C. Lin, "Design of a leg-wheel hybrid mobile platform," in *2009 IEEE/RSJ International Conference on Intelligent Robots and Systems*, 2009, pp. 4682–4687.
- [5] Y.-S. Kim, G.-P. Jung, H. Kim, K.-J. Cho, and C.-N. Chu, "Wheel Transformer: A Wheel-Leg Hybrid Robot With Passive Transformable Wheels," *IEEE Trans. Robot.*, vol. 30, no. 6, pp. 1487–1498, Dec. 2014.
- [6] S. Jacobsen, F. M. Smith, M. Olivier, and C. S. Maggio, "(12) United States Patent," US 7,017,687 B1, 2006.
- [7] S. K. Saha and T. Mcgraw-hill, "Denavit and Hartenberg (DH) Parameters Fixed Base End-effector," in *Introduction to Robotics*, New Delhi, 2010, pp. 1–7.